Solution-Processed Fullerene-Based Organic Schottky Junction Devices for Large-Open-Circuit-Voltage Organic Solar Cells

Bin Yang, Fawen Guo, Yongbo Yuan, Zhengguo Xiao, Yunzhang Lu, Qingfeng Dong, and Jinsong Huang*

With their rapidly rising power conversion efficiency (*PCE*) in the last decade, organic photovoltaic devices (OPVs) are now seriously considered as a candidate for low-cost solar-energy-conversion applications. Nevertheless, the *PCE* of OPVs is still lower than that of the dominating silicon photovoltaic cells or other thin-film photovoltaic technologies. In order to push the *PCE* to 15% for its successful commercialization, an attractive strategy is to improve the open-circuit voltage (V_{oc}) without losing other photovoltaic parameters such as the short-circuit current (J_{sc}) and the fill factor (*FF*). Currently, all efficient OPVs are based on bulk heterojunctions (BHJs) in which a donor and an acceptor are mixed to split the light-generated high-binding-energy Frenkel excitons.[1–6] The V_{oc} of BHJ OPVs is determined by the energy difference between the lowest unoccupied molecular orbital (LUMO) of the acceptor and the highest occupied molecular orbital (HOMO) of the donor.[7] The broadly applied strategy to increase the V_{oc} in BHJ OPVs is to lift the LUMO of the acceptor and/or to shift down the HOMO of the donor by molecular design[5,8] or energy-level tuning with an inserted dipole layer.[9] There is a trade-off between the charge-transfer efficiency and the V_{oc} in BHJ OPVs: a large energy offset between the LUMO of the donor and the acceptor is required for efficient charge transfer and separation, which would squeeze the V_{oc}.[10] Despite the recent encouraging discovery that the LUMO offset between the donor and the acceptor can be as small as 0.12 eV for efficient charge transfer,[11] most high-efficiency donor/acceptor systems generally have a large LUMO offset of 0.6–1 eV,[4,12–15] which limits the V_{oc} to be much smaller than the polymer's optical bandgap (E_g).[10]

We recently found that the OPV devices with only a fullerene (C_{60} and its derivatives, that is, [6,6]-phenyl-C_{61}-butyric acid methyl ester (C_{60}-PCBM) and indene-C_{60} bisadduct (C_{60}-ICBA)) as the active layer can output a V_{oc} of 0.83–0.95 V. These devices have a simple device structure of indium tin oxide (ITO)/poly(3,4-ethylenedioxythiophene):poly(styrene sulfonate) (PEDOT:PSS)/fullerene/bathocuproine (BCP)/aluminum (Al).

The photocurrents of these devices under AM 1.5G simulated illumination at 100 mW cm^{-2} are shown in **Figure 1**a. Since the donor material is completely absent in the active layers, the BHJ working mechanism does not apply for these devices. Since fullerenes are slightly doped *n*-type semiconductors with a reasonably high electron concentration of 10^{17}–10^{18} cm^{-3},[16] the Schottky barrier is expected to form at the fullerene/PEDOT:PSS contact with a sizable band bending in the fullerene. An energy diagram for these fullerene Schottky-junctions is plotted in Figure 1b, which shows that the high V_{oc} of these fullerene-only devices arises from the Fermi energy-difference-induced band bending in the fullerene close to the fullerene/PEDOT:PSS contact.[17–19] Since the work function of the anode is easily tuned with previously established surface modification,[20] a high V_{oc} is therefore expected by the combination of the high work function of the anode with the low LUMO energy level of the semiconductor.

It is noted that the V_{oc} of Schottky junction devices, around 0.83 V for the C_{60}-PCBM-based device, is much larger than that of many BHJ devices, such as P3HT:C_{60}-PCBM-based BHJ devices. Since band bending at the Schottky junction is determined by the Fermi energy difference between the anode and the fullerene, a varied Fermi energy of fullerene materials should tune the band bending and thus the V_{oc} of Schottky junction devices.[21] In this work, three fullerene family materials, C_{60}, C_{60}-PCBM, and C_{60}-ICBA, were studied. The LUMOs of C_{60}, C_{60}-PCBM and C_{60}-ICBA are 4.5 eV,[22] 3.9 eV,[8,21] and 3.7 eV,[8,21] respectively, and the HOMOs are almost the same ($\approx$6.1 eV), as shown in Figure 1b. It is obvious that the variation trend of the obtained V_{oc} follows that of the LUMOs of the fullerene materials (Figure 1a). The highest obtained V_{oc} was 0.95 V, which was achieved by the C_{60}-ICBA-based Schottky junction devices. The V_{oc} of the C_{60}-PCBM devices can be further increased to 0.87 V by increasing the work function of the anode using thermally deposited molybdenum oxide (MoO$_3$) on an ITO substrate.

The weak electric field in the Schottky junction should not provide enough driving force for the separation of photogenerated Frenkel excitons in organic semiconductor materials because the Frenkel excitons have too large a binding energy, of the order of 0.4–1 eV, to be separated by the weak electric field in regular OPVs.[23–26] Early studies of Schottky junction-based organic solar cells gave a very small photocurrent on the order of $\approx$10 µA cm^{-2}.[27,28] While these fullerene-only Schottky junction devices can output a J_{sc} on the order of 1 mA cm^{-2}, which is 1–2 orders magnitude larger than those Schottky junction devices

B. Yang, F. Guo, Dr. Y. Yuan, Z. Xiao, Y. Lu, Q. Dong, Prof. J. Huang
Department of Mechanical and Materials Engineering and Nebraska Center for Materials and Nanoscience
University of Nebraska–Lincoln
Lincoln, NE 68588-0656, USA
E-mail: jhuang2@unl.edu

Materials
Views
www.MaterialsViews.com

ADVANCED
MATERIALS
www.advmat.de

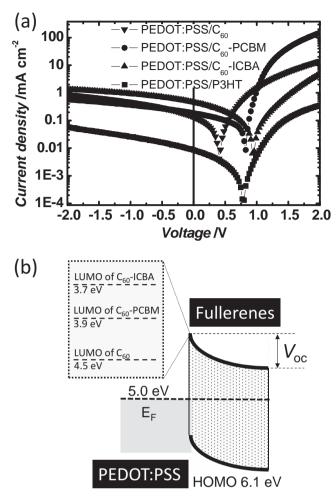COMMUNICATION

(a)

(b)

Figure 1. a) J–V curves of C_{60}-, C_{60}-PCBM- and C_{60}-ICBA-based Schottky junction devices. b) Schematic energy diagram showing the variation of V_{oc} of C_{60}-, C_{60}-PCBM- and C_{60}-ICBA-based Schottky junction devices. For better clarity, the energy levels were not drawn in scale.

with conjugated polymers such as poly(3-hexylthiophene) (P3HT) as the active layer, as shown in Figure 1a. The relatively large photocurrent output from fullerene-based Schottky junction devices can be understood by the delocalization of electrons in the fullerene aggregates.[29–31] The delocalization of electrons in fullerene aggregates is caused by the coherent intermolecular electron transfer between fullerene molecules[29] on the timescale of 60 fs,[32] which stabilizes the molecules, results in long-lifetime polarons, and reduces the energy barrier for electron transfer.[29] The intermolecular charge transfer excitons (CTEs), formed by electron transfer between the fullerene molecules, have a bandgap of 2.3–4.0 eV,[30,33] which is significantly larger than the Frenkel exciton bandgap of 1.5–1.9 eV.[33] The CTE binding energy is thus much smaller than that of the Frenkel excitons in a fullerene. A small binding energy of 25 meV for CTEs in fullerene was derived by an electric-field-assisted photoluminescence quench study.[33] The electron delocalization diameter derived from such a small CTE binding energy is around 10 nm, which is consistent with the

quantum-dynamics calculation result that electrons delocalize over several molecules in fullerene aggregates.[29] Therefore, photogenerated excitons can be separated at a relatively small electric field of 10^5 V cm^{-1}, which results in a strong photo-conductivity of fullerene materials at room temperature.[34] The built-in electric field on the order of 10^5 V cm^{-1}, which is induced by the Fermi energy level difference between the anode and the fullerene, is then high enough to separate the intermolecular CTEs in the fullerene and results in a reasonable large photocurrent in fullerene-only Schottky junction devices. It is noted that the delocalization of electrons in the aggregates and the small CTE exciton binding energy are also considered to be responsible for fast diffusion of excitons in the crystalline C_{60}-PCBM domain,[35] the efficient dissociation of charge-transfer excitons at polymer/fullerene interface,[36] and the highest-reported field-effect mobility of 8–11 cm^2 V^{-1} s^{-1}[37,39] in fullerene field-effect transistors.

The photocurrent in fullerene-only-based Schottky junction devices is still low (**Figure 2**a), compared with that of most BHJ devices.[9,40] One reason is that the bandgap of CTEs of ≈2.3 eV is too large, so that only a small portion of absorbed sunlight can yield photocurrent. The lower-energy Frenkel excitons still cannot be split and do not contribute to the photocurrent. This is confirmed by the measured external quantum efficiency (EQE) of pure-fullerene-based Schottky junction devices, as shown in Figure 2b. The EQE dramatically drops to almost zero at a wavelength of 532 nm which coincides with the bandgap of CTE (2.3 eV). Another reason for the low photocurrent and EQE from the fullerene-only-based Schottky junction devices should be the very low hole mobility in the fullerene, which causes severe charge recombination due to inefficient hole extraction. To address this issue and enhance the absorption, a small amount of hole-transporting polymer, 5 wt% of P3HT was added into [6,6]-phenyl-C_{71}-butyric acid methyl ester (C_{70}-PCBM). Strikingly, the addition of a low concentration of donor material does not impair the large V_{oc} in Schottky junction devices, while significantly increasing the J_{sc} to 9–10 mA cm^{-2}, which is comparable to that of optimized P3HT:C_{70}-PCBM-based BHJ devices (Figure 2a). The EQE of approximately 64%, as shown in Figure 2b, is also comparable to that of BHJ devices. The small P3HT loading ratio of 5 wt% contributes a negligible light absorption, which is shown by the almost-identical transmission-absorption spectra of the C_{70}-PCBM-only film and the 5 wt% P3HT-doped C_{70}-PCBM film (Figure 2c). The large photocurrent observed here should be ascribed to the very strong absorption coefficient of C_{70}-PCBM. To include the optical-interference effect, the absolute absorption spectra of the Schottky junction devices were measured using the reflection method, as described elsewhere.[34] As shown in Figure 2d, the maximum absorption of the C_{70}-PCBM film in the Schottky junction device reaches 90% and the absorption is above 60% in a broad wavelength range above its optical bandgap. Again, the reflective-absorption spectra of the C_{70}-PCBM-only film and the 5 wt% P3HT-doped C_{70}-PCBM film are almost identical. We also observed a significant increased internal quantum efficiency (IQE) of 80% in the device with the 5 wt% P3HT-doped C_{70}-PCBM film (Figure 2d), which is close to the calculated IQE of ≈85% by measuring the saturated EQE under a reverse bias of −2 V to extract all of the photogenerated charges (Figure 2e). Despite the doped small amount of P3HT
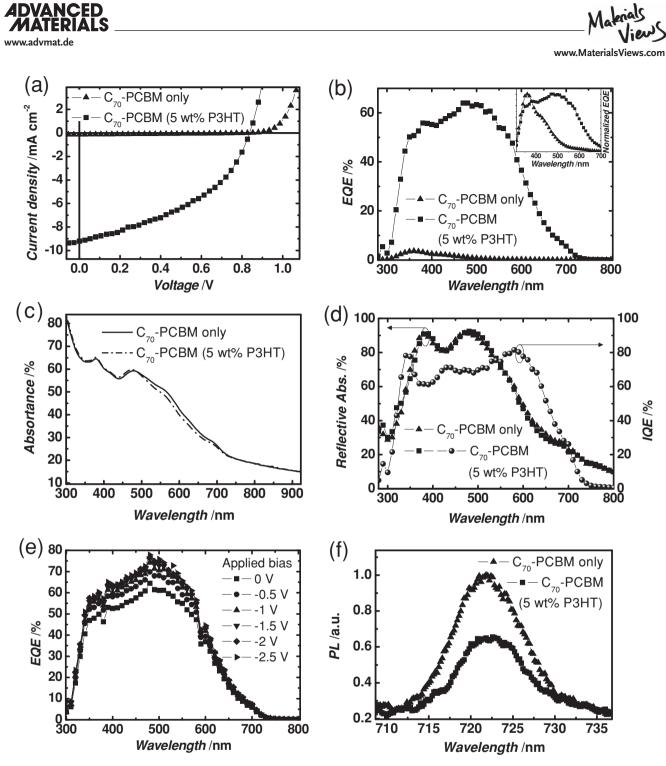
COMMUNICATION

Figure 2. a,b) The photocurrent curves (a) and EQE curves (b) of Schottky junction devices based on pure C$_{70}$-PCBM and C$_{70}$-PCBM:P3HT (95 wt%:5 wt%). c) The transmission absorption spectra of C$_{70}$-PCBM-only film and the blend film C$_{70}$-PCBM:P3HT (95 wt%:5 wt%). d) The IQE (right) and reflective absorption spectra (left) of C$_{70}$-PCBM-only- and C$_{70}$-PCBM:P3HT (95 wt%:5 wt%)-based devices. e) The EQE curves of the Schottky junction device based on C$_{70}$-PCBM:P3HT (95 wt%:5 wt%) under different reverse biases. f) The PL spectra of the C$_{70}$-PCBM-only film and the C$_{70}$-PCBM:P3HT (95 wt%:5 wt%) blend film.

not contributing to light absorption, it significantly increases the device efficiency by increasing the Frenkel exciton dissociation and forming a hole-percolation path in the C$_{70}$-PCBM matrix for efficient hole extraction. The normalized EQE curve of the devices with 5 wt% P3HT-doped C$_{70}$-PCBM is totally different to

that of the C$_{70}$-PCBM-only-based device, as shown in the inset of Figure 2b. The expansion of the EQE cut-off from 532 nm to 700 nm indicates that the Frenkel excitons from C$_{70}$-PCBM in the Schottky junction device with the doped P3HT also contribute to the photocurrent, in addition to the CTEs. This was confirmed
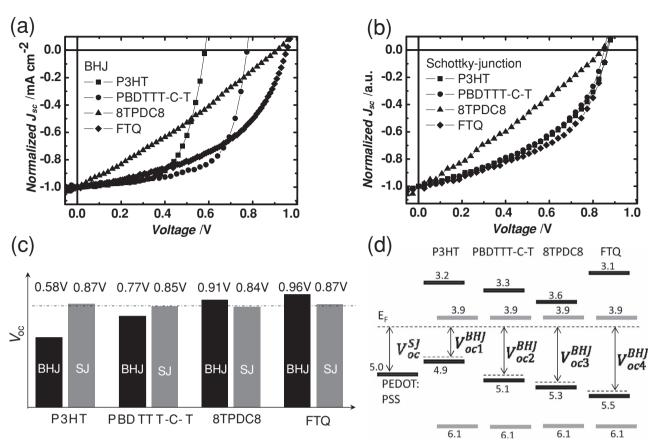
Figure 3. a,b) Normalized photocurrent curves of the BHJ devices (a) for different donors and Schottky junction (SJ) devices (b) for different donors, with donor polymers P3HT (50 wt% for BHJ, 5 wt% for SJ), PBDTTT-C-T (50 wt% for BHJ, 5 wt% for SJ), 8TPDC8 (50 wt% for BHJ, 5 wt% for SJ), and FTQ (40 wt% for BHJ, 5 wt% for SJ). c) The measured V_{oc} of SJ and BHJ devices. d) Comparison of the energy diagram of V_{oc} determined by SJ and BHJ; the black bars represent the donor materials, the grey bars represent C_{70}-PCBM.

by the photoluminescence (PL) quenching study, as shown in Figure 2f. The 5 wt% P3HT doping in the C_{70}-PCBM can reduce the PL of the C_{70}-PCBM by almost half through photoinduced electron transfer from the P3HT to the C_{70}-PCBM.

The Mott–Schottky analysis of the capacitance–voltage measurement result gives an almost-constant carrier concentration around 1.0×10^{17} cm^{-3} in the C_{70}-PCBM material before and after doping with a low concentration of 5 wt% P3HT, as shown in Figure S1 in the Supporting Information, which is consistent with the reported value as mentioned previously.[16] The Fermi energy level of C_{70}-PCBM was then calculated to be about 0.2 eV below the LUMO of C_{70}-PCBM, which is approximately 4.1 eV below the vacuum level. The Fermi energy difference of 0.9 eV between PEDOT:PSS and C_{70}-PCBM agrees well with the experimentally obtained V_{oc} of 0.8–0.9 V (Figure 2a). The depletion widths for both the pure C_{70}-PCBM film device and the 95 wt% C_{70}-PCBM:5 wt% P3HT device are almost the same, approximately 80 nm, because the carrier concentration is unchanged. Since the depletion width is much larger than the active film thickness of 55 nm, the band bending is able to extend to the entire active film as depicted in Figure 1b, which helps efficient charge extraction.

It is noted that a large increase in V_{oc} with a low donor doping concentration has been observed in several other material

systems by several other groups.[41,42] However, in these studies the devices with low donor concentration were still believed to work with the BHJ mechanism, and the high V_{oc} was explained by a reduced reverse saturated dark current.[42] Recently, Tang and co-workers reported that a small loading of several donors in a C_{70} active layer in devices with MoO$_x$ as the anode could produce a much-larger V_{oc} than a large loading of donor.[43] It was proposed that the V_{oc} might be determined by the barrier at MoO$_x$/BHJ interface instead of the BHJ mechanism.[43] Nevertheless, there was no clear evidence to support this claim to exclude the BHJ mechanism. It is still possible that the large V_{oc} in Tang's devices with low donor loading might follow the rule of the BHJ device because a diluted donor in C_{70} should result in a lowered HOMO of the donor and thus a larger V_{oc}. In this work, firstly, we excluded the possibility of a reduced reverse saturated dark current because no obvious dark-current reduction was observed in our devices with low P3HT doping concentration, compared with those devices with a high P3HT doping concentration. Secondly, the following three phenomena exclude the possibility of the BHJ mechanism and confirm that the V_{oc} in the fullerene-based Schottky junctions is only determined by the Fermi level of the fullerene and the PEDOT:PSS. Firstly, we reduced the P3HT loading ratio from 5 wt% to 1 wt%, which should further push down the HOMO of the

P3HT, since the down-shift of HOMO of P3HT was observed previously.[44] However, the V_{oc} remained unchanged and did not follow the variation of HOMO. Secondly, we tested four donor materials with different HOMO energy levels, including P3HT, poly[4,8-bis-substituted-benzo[1,2-b:4,5-b']dithiophene-2,6-diyl-*alt*-4-substituted-thieno[3,4-b]thiophene-2,6-diyl] (PBDTTT-C-T),[45] 5-(2,6-bis((E)-2-(3,4-dioctyl-[2,2':5',2'':5'',2'''-quaterthiophen]-5-yl)vinyl)-4H-pyran-4-ylidene)-1,3-diethyl-2-thioxodihydropyrimidine-4,6 (1H, 5H)-dione (8TPDC8) and fluorine-substituted poly[2,3-bis-(3-octyloxyphenyl) quinoxaline-5,8-diyl-alt-thiophene-2,5-diyl] (FTQ), whose chemical structures are shown in Figure S2 in the Supporting Information. In order to compare conveniently the V_{oc} difference among these four kinds of donors in the BHJ and Schottky junction devices, the obtained J–V curves under simulated AM 1.5G illumination were normalized, as shown in the **Figure 3**a,b. Despite these donor materials having completely different V_{oc} values in BHJ devices (with donor loading ranges from 40–50 wt%), varying from 0.58 V to 0.96 V, all of the devices with 5 wt% donor as the active layer show almost the same V_{oc}, around 0.86 V, which is irrespective of the HOMO of the donor molecules. Thirdly, the HOMO levels for FTQ and 8TPDC8 are so low that the V_{oc} of 0.91–0.96 V in a BHJ is larger than the Schottky junction V_{oc} of 0.86 V. A smaller donor loading ratio of 5 wt% should lead to an even larger V_{oc} if the V_{oc} is determined by the BHJ mechanism. Therefore, as summarized in Figure 3c,d, the V_{oc} in a fullerene-based Schottky junction is only governed by the work function of the PEDOT:PSS and the Fermi level of the fullerene, which is different to the BHJ devices whose V_{oc} should be determined by the HOMO of the donor material.

The 95 wt% C_{70}-PCBM: 5 wt% P3HT-based Schottky junction devices have an efficiency of 3.3% under simulated AM 1.5G illumination at 100 mW cm^{-2}. There is still a strong charge recombination in the present Schottky junction device due to the unoptimized hole extraction, which is reflected by the increased photocurrent output at reverse bias and the low FF of the Schottky junction devices, as shown in the Figure 2a. To understand the recombination mechanism in the fullerene-based Schottky junction device, the light-intensity dependence of the photocurrent output was measured under illumination from 0.001 Sun to 3 Suns. The variation in V_{oc} with incident light intensity is shown in **Figure 4**. It is clear that the V_{oc} increases linearly with light intensity [ln(I)]. The linear fitting result shows that the slope is approximately equal to $k_B T/e$ (here, k_B is the Boltzmann constant, T is temperature, and e is the element electron charge), indicating the main recombination mechanism is bimolecular recombination at the open circuit in the fullerene-based Schottky junction devices.[46] As shown in the Figure 4, the responsivity decreases continuously with increasing light intensity. The FF is maintained constant at low light intensity below 2 mW cm^{-2} and then decreases with further increased light intensity. The reduced responsivity and FF under strong light indicates again the existence of significant charge recombination in this Schottky junction device. The PCE increases to 5% at low light intensity, below 2 mW cm^{-2}, due to the reduced charge recombination, which is higher than that of BHJ devices. The high efficiency at low light intensity makes it ideal for the application of indoor light-energy harvesting. Compared with the thermally evaporated
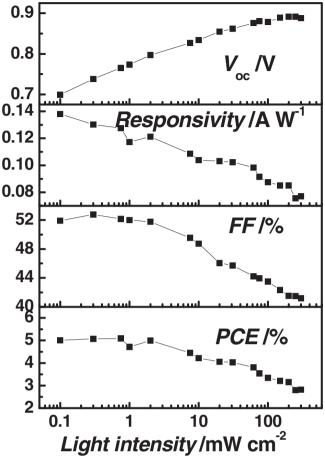

Figure 4. The variation of the photovoltaic parameters with light intensity for the Schottky junction device with C_{70}-PCBM:P3HT (95:5 wt%) as the active layer.

C_{70}-based devices, as reported by Tang and co-workers,[43] the solution-processed Schottky junction devices reported here are simpler to fabricate, and are compatible with large-scale, low-cost fabrication methods such as spray-coating and the roll-to-roll fabrication process.

In conclusion, a high V_{oc} of 0.95 V was obtained in the fullerene-based Schottky junction devices. The V_{oc} is expected to be even higher by the combination of a higher work function of the anode and a lower LUMO energy level of the fullerene. The PCE of the C_{70}-PCBM:P3HT (95:5 wt%) Schottky junction device reaches 5% at low light intensity, higher than that of the corresponding BHJ devices. This is the highest-reported efficiency in solution-processed Schottky junction devices. An additional potential advantage of using Schottky junction devices is that the low concentration of the donor polymer makes it more stable, likely due to the more-stable morphology with less donor-polymer aggregation. The device stability is still under study.

Experimental Section

Approximately 10 min of plasmonic treatment was conducted on cleaned ITO/glass substrates using UV-ozone. Subsequently, the PEDOT:PSS (Baytron-P 4083, used as received) was spin-coated onto

it at a spinning speed of 3500 rpm., which produced a PEDOT:PSS film thickness of approximately 30 nm, as measured with a Dektak profilometer. The obtained PEDOT:PSS film was baked at 125 °C for 30 min. Subsequently, the mixture solution (concentration of 35 mg mL^{-1}) with different compositions of P3HT (Rieke, used as received) in C$_{70}$-PCBM, which was pre-dissolved in chlorobenzene, was spin-coated onto PEDOT:PSS film at a spinning speed of 4000 rpm for 20 s to form a layer thickness of approximately 55 nm (measured with a Dektak profilometer). Then, the obtained film was annealed at 110 °C for 10 min in a nitrogen-filled glovebox. Finally, a layer of 7 nm-thick BCP, which was covered by 100 nm-thick Al, was obtained by thermal evaporation, as a cathode. The active device area was approximately 0.07 cm^2.

The absorption measurements were conducted using an Evolution 201 UV–visible spectrophotometer (Thermo Scientific). The PL spectra were obtained by using a commercial spectrophotometer (F-4500, Hitachi Inc.) equipped with a standard solid sample holder. The excitation light was provided by a xenon lamp and restricted to a spectral window of 480 ± 2.5 nm. To minimize the measurement error, all of the films were spin-coated on precleaned silica glass substrates.

Supporting Information

Supporting Information is available from the Wiley Online Library or from the author.

Acknowledgements

[1] S. R. Forrest, *MRS Bull.* **2005**, *30*, 28.
[2] G. Li, V. Shrotriya, J. Huang, Y. Yao, T. Moriarty, K. Emery, Y. Yang, *Nat. Mater.* **2005**, *4*, 864.
[3] A. C. Mayer, S. R. Scully, B. E. Hardin, M. W. Rowell, M. D. McGehee, *Mater. Today* **2007**, *10*, 28.
[4] S. H. Park, A. Roy, S. Beaupré, S. Cho, N. Coates, J. S. Moon, D. Moses, M. Leclerc, K. Lee, A. J. Heeger, *Nat. Photon.* **2009**, *3*, 297.
[5] C. E. Small, S. Chen, J. Subbiah, C. M. Amb, S.-W. Tsang, T.-H. Lai, J. R. Reynolds, F. So, *Nat. Photon.* **2012**, *6*, 115.
[6] Y. Sun, G. C. Welch, W. L. Leong, C. J. Takacs, G. C. Bazan, A. J. Heeger, *Nat. Mater.* **2012**, *11*, 44.
[7] C. J. Brabec, A. Cravino, D. Meissner, N. S. Sariciftci, T. Fromherz, M. T. Rispens, L. Sanchez, J. C. Hummelen, *Adv. Funct. Mater.* **2001**, *11*, 374.
[8] Y. He, H. Y. Chen, J. Hou, Y. Li, *J. Am. Chem. Soc.* **2010**, *132*, 1377.
[9] B. Yang, Y. Yuan, P. Sharma, S. Poddar, R. Korlacki, S. Ducharme, A. Gruverman, R. Saraf, J. Huang, *Adv. Mater.* **2012**, *24*, 1455.
[10] G. Dennler, M. C. Scharber, C. J. Brabec, *Adv. Mater.* **2009**, *21*, 1323.
[11] X. Gong, M. Tong, F. G. Brunetti, J. Seo, Y. Sun, D. Moses, F. Wudl, A. J. Heeger, *Adv. Mater.* **2011**, *23*, 2272.
[12] C. M. Amb, S. Chen, K. R. Graham, J. Subbiah, C. E. Small, F. So, J. R. Reynolds, *J. Am. Chem. Soc.* **2011**, *133*, 10062.
[13] S. C. Price, A. C. Stuart, L. Yang, H. Zhou, W. You, *J. Am. Chem. Soc.* **2011**, *133*, 4625.
[14] Z. He, C. Zhong, X. Huang, W.-Y. Wong, H. Wu, L. Chen, S. Su, Y. Cao, *Adv. Mater.* **2011**, *23*, 4636.
[15] Y. Liang, Z. Xu, J. Xia, S. T. Tsai, Y. Wu, G. Li, C. Ray, L. Yu, *Adv. Mater.* **2010**, *22*, E135.
[16] B. Ecker, J. C. Nolasco, J. Pallarés, L. F. Marsal, J. Posdorfer, J. Parisi, E. Von Hauff, *Adv. Funct. Mater.* **2011**, *21*, 2705.
[17] P. P. Boix, J. Ajuria, I. Etxebarria, R. Pacios, G. Garcia-Belmonte, J. Bisquert, *J. Phys. Chem. Lett.* **2011**, *2*, 407.
[18] A. J. Morfa, A. M. Nardes, S. E. Shaheen, N. Kopidakis, J. van de Lagemaat, *Adv. Funct. Mater.* **2011**, *21*, 2580.
[19] S. M. Sze, K. K. Ng, *Physics of Semiconductor Devices*, Third edition, John Wiley & Sons, Inc., Hoboken, NJ, USA **2007**.
[20] A. Petr, F. Zhang, H. Peisert, M. Knupfer, L. Dunsch, *Chem. Phys. Lett.* **2004**, *385*, 140.
[21] A. Guerrero, L. F. Marchesi, P. P. Boix, J. Bisquert, G. Garcia-Belmonte, *J. Phys. Chem. Lett.* **2012**, *3*, 1386.
[22] S. Yoo, B. Domercq, B. Kippelen, *Appl. Phys. Lett.* **2004**, *85*, 5427.
[23] S. Alvarado, P. Seidler, D. Lidzey, D. Bradley, *Phys. Rev. Lett.* **1998**, *81*, 1082.
[24] S. Barth, H. Bässler, *Phys. Rev. Lett.* **1997**, *79*, 4445.
[25] K. Sakurai, H. Tachibana, N. Shiga, C. Terakura, M. Matsumoto, Y. Tokura, *Phys. Rev. B* **1997**, *56*, 9552.
[26] Y. He, G. Zhao, B. Peng, Y. Li, *Adv. Funct. Mater.* **2010**, *20*, 3383.
[27] S. Karg, W. Riess, V. Dyakonov, M. Schwoerer, *Synth. Met.* **1993**, *54*, 427.
[28] S. Rajaputra, G. Sagi, V. P. Singh, *Sol. Energy Mater. Sol. Cells* **2009**, *93*, 60.
[29] H. Tamura, M. Tsukada, *Phys. Rev. B* **2012**, *85*, 054301.
[30] S. Cook, H. Ohkita, Y. Kim, J. J. Benson-Smith, D. D. C. Bradley, J. R. Durrant, *Chem. Phys. Lett.* **2007**, *445*, 276.
[31] R. Munn, B. Pac, P. Petelenz, *Phys. Rev. B* **1998**, *57*, 1328.
[32] J. Jakowski, S. Irle, B. G. Sumpter, K. Morokuma, *J. Phys. Chem. Lett.* **2012**, *3*, 1536.
[33] S. Kazaoui, R. Ross, N. Minami, *Phys. Rev. B* **1995**, *52*, R11665.
[34] J. Huang, Y. Yang, *AppL. Phys. Lett.* **2007**, *91*, 203505.
[35] S. R. Cowan, N. Banerji, W. L. Leong, A. J. Heeger, *Adv. Funct. Mater.* **2012**, *22*, 1116.
[36] A. A. Bakulin, A. Rao, V. G. Pavelyev, P. van Loosdrecht, M. S. Pshenichnikov, D. Niedzialek, J. Cornil, D. Beljonne, R. H. Friend, *Science* **2012**, *335*, 1340.
[37] H. Li, B. C. K. Tee, J. J. Cha, Y. Cui, J. W. Chung, S. Y. Lee, Z. Bao, *J. Am. Chem. Soc.* **2012**, *134*, 2760.
[38] T. B. Singh, N. S. Sariciftci, H. Yang, L. Yang, B. Plochberger, H. Sitter, *Appl. Phys. Lett.* **2007**, *90*, 213512.
[39] H. Bräuning, R. Trassl, A. Diehl, A. Theiß, E. Salzborn, A. Narits, L. Presnyakov, *Phys. Rev. Lett.* **2003**, *91*, 168301.
[40] B. Yang, J. Cox, Y. Yuan, F. Guo, J. Huang, *Appl. Phys. Lett.* **2011**, *99*, 133302.
[41] J. Sakai, T. Taima, K. Saito, *Org. Electron.* **2008**, *9*, 582.
[42] G. Wei, S. Wang, K. Renshaw, M. E. Thompson, S. R. Forrest, *ACS Nano* **2010**, *4*, 1927.
[43] M. Zhang, H. Wang, H. Tian, Y. Geng, C. W. Tang, *Adv. Mater.* **2011**, *23*, 4960.
[44] W. C. Tsoi, S. J. Spencer, L. Yang, A. M. Ballantyne, P. G. Nicholson, A. Turnbull, A. G. Shard, C. E. Murphy, D. D. C. Bradley, J. Nelson, J.-S. Kim, *Macromolecules* **2011**, *44*, 2944.
[45] L. Huo, S. Zhang, X. Guo, F. Xu, Y. Li, J. Hou, *Angew. Chem. Int. Ed.* **2011**, *50*, 9697.
[46] S. R. Cowan, A. Roy, A. J. Heeger, *Phys. Rev. B* **2010**, *82*, 245207.